JOURNAL OF PROPULSION AND POWER
Vol. 12, No. 4, July–August 1996

Analysis of Partially Mixed Supersonic Ejector

Dimitri Papamoschou*
University of California, Irvine, Irvine, California 92717

This article presents an analytical model of a supersonic/subsonic, constant-area ejector whose exit flow is not uniformly mixed. The primary and secondary streams, separated by the dividing streamline, are treated as quasi-one-dimensional. The shear stress on the dividing streamline, the resulting heat transfer, and the wall stresses are applied artificially on the streams. Axisymmetric and two-dimensional configurations are considered. The model predicts that the axisymmetric ejector provides better thrust augmentation than the two-dimensional one, the latter suffering from higher skin-friction losses. Thrust increases with ejector length, but at a diminishing rate. For all configurations, thrust augmentation decreases with flight Mach number and becomes zero at a flight Mach number of about 0.7. Increasing the primary-to-secondary area ratio has a minimal effect on thrust. The results compare favorably with available experimental data on pressure distributions and mass-flow ratios.

Nomenclature

A = cross-sectional area
a = speed of sound
b = ejector radius (A/S) or half-height (two dimensional)
c_p = specific heat at constant pressure
H = total enthalpy
h = static enthalpy
l = length scale, Eq. (11)
M = Mach number
M_c = convective Mach number
$\dot{m}$ = mass flux
p = pressure
q = heat transfer
R = gas constant
r = velocity ratio, $U_{\infty 1}/U_{\infty 2}$
$\dot{S}$ = entropy flux
s = entropy
T = temperature
U = velocity
x = streamwise coordinate
y = transverse coordinate
γ = specific-heat ratio
ΔU = $U_{\infty 1} - U_{\infty 2}$
δ_ω = shear-layer vorticity thickness
η = density ratio, $\rho_{\infty 1}/\rho_{\infty 2}$
μ = viscosity
ρ = density
τ = shear stress

Subscripts
a = ambient
e = ejector exit, $x = L$
i = ejector inlet, $x = 0$
T = total, stagnation
w = wall
1 = primary stream
2 = secondary stream
$*$ = dividing streamline
∞ = isentropic freestream

Received Aug. 18, 1995; revision received Jan. 30, 1996; accepted for publication Feb. 8, 1996.

*Associate Professor, Department of Aerospace and Mechanical Engineering. Member AIAA.

Introduction

EJECTORS are modified nozzles for the purpose of augmenting thrust and suppressing exhaust noise. The latter application is particularly relevant to the high-speed civil transport that needs to be much quieter than today's supersonic transports to meet Federal Aviation Administration (FAA) Stage III noise regulations. Analytical treatments of ejectors are based on von Kármán's[1] approach in which the flow exiting the ejector is assumed fully mixed and uniform. Exact solutions for the exit conditions yield the thrust augmentation and pumping efficiency. For large ejector areas, von Kármán's approach predicts thrust augmentation on the order of 100% (see Ref. 2).

For supersonic jets, the uniformly mixed assumption becomes unrealistic. At high Mach numbers, the jet growth rate is very slow, requiring long ejector lengths to achieve fully mixed exit conditions. This is practically unfeasible because of the weight and thrust penalties. Experimental data in relatively long ejectors show that the flow is far from being fully mixed at the exit.[3] Mixing enhancement[4,5] shortens the ejector length required for a certain amount of mixed fluid at the exit, but even then it is unlikely that the exit flow would be uniformly mixed. In fact, it is not necessary to have a fully mixed exhaust for the ejector to provide considerable thrust benefit, as this analysis will show. It is important to have an analytical model for ejectors with partially mixed exhaust. This article presents the development of such a model and demonstrates its use in a parametric evaluation of ejector performance.

Quasi-One-Dimensional Model

We consider an ejector supplied by a supersonic primary stream and having a constant-area, thin, and adiabatic shroud. Both primary and secondary streams consist of air. The analysis treats the ejector shear layer as composed of two quasi-one-dimensional streams. The transformation from the y dependent to the quasi-one-dimensional variables is illustrated in Fig. 1. In both settings, the static pressure is assumed uniform in the crossplane direction, $p = p(x)$. The two streams are separated by the dividing streamline y_*, hence, each stream preserves its $\dot{m}$. The shape of the dividing streamline is initially unknown and is found by the computational scheme described herein.

The y-dependent Mach number profile is replaced by two uniform Mach numbers, M_1 and M_2. The same occurs with all the other variables. Even though we lose the details of the transverse gradients of velocity and temperature, we retain the main effects of those gradients, namely the shear stresses and heat transfer, which are now artificially applied on the quasi-

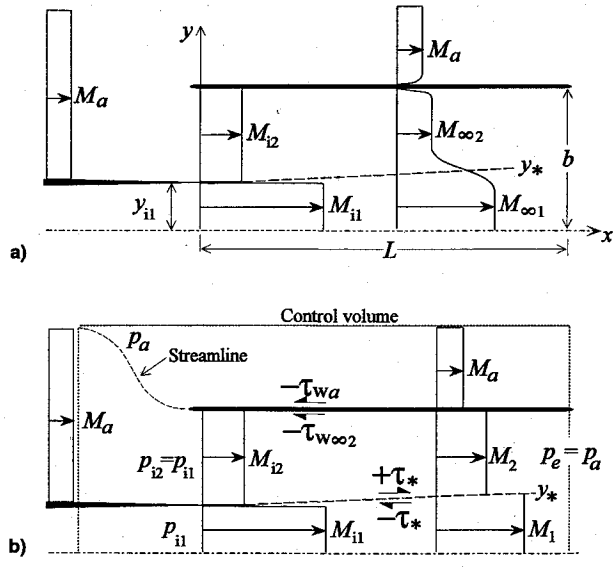

Fig. 1 Sketch of ejector model depicting a) the Mach number profiles and b) the quasi-one-dimensional simplification. Also shown is control volume used to calculate the ejector thrust.

one-dimensional flowfield. The application of the shear stresses is shown in Fig. 1: for the primary stream, the stress $-\tau_*$ on the dividing streamline opposes the fluid motion. For the slow stream, the equal and opposite stress $+\tau_*$ acts towards the flow direction (it can be thought of as negative friction), whereas a wall stress $-\tau_{w\infty 2}$ acts on the inner surface of the ejector shroud. It is the $+\tau_*$ stress that generates the secondary stream by dragging ambient air into the ejector. For the two-dimensional ejector, additional wall stresses act on the sidewalls. In the y-dependent description, the flow external to the shear layer and boundary layers (freestream flow) is assumed isentropic. This is important, because the shear stresses depend on the freestream quantities and not on the averaged quasi-one-dimensional quantities.

The shear stress on the dividing streamline τ_* is an essential element of the model and is estimated by the methods in Ref. 6, which the reader may wish to consult for more details on the quasi-one-dimensional approximation. First, we define the convective Mach number,

$$M_c = \frac{\Delta U}{a_{\infty 1} + a_{\infty 2}} \tag{1}$$

which is a measure of the intrinsic compressibility of the shear layer. The shear stress on the dividing streamline is

$$\tau_* = K\frac{1}{2}(\rho_{\infty 1} + \rho_{\infty 2})(\Delta U)^2\left[\frac{(1+r)(1+\eta)}{2(1+r\eta)}\right]f(M_c) \tag{2}$$

where K is an empirical constant, obtained from subsonic constant-density experiments. Here we use Wygnanski and Fiedler's[7] value $K = 0.013$. The term inside the brackets represents the effect of density ratio, while $f(M_c)$ accounts for the compressibility effect. The growth rate of the vorticity thickness (about half of the visual thickness) is

$$\frac{d\delta_w}{dx} = 0.085\frac{(1+\eta)(1-r)}{1+r\eta}f(M_c) \tag{3}$$

The vorticity thickness is used here to define the edges of the shear layer within which the flow is dominated by viscous effects. Outside those edges, the flow is assumed to be potential. The function $f(M_c)$ describes the effect of compressibility to suppress the growth rate, hence the shear stress, and is approximated by

$$f(M_c) \approx 0.25 + 0.75e^{-3M_c^2} \tag{4}$$

To obtain the wall stresses, we use Van Driest's[8] formula for the skin-friction coefficient c_f:

$$0.242\sqrt{(1-\lambda^2)/c_f}(\sin^{-1}\lambda/\lambda) = \log(R_x c_f) + 1.26\log(1-\lambda^2) \tag{5}$$
$$1 - \lambda^2 = \{1 + [(\gamma-1)/2]M_\infty^2\}^{-1}$$

where R_x is the Reynolds number based on streamwise distance x and the relation $\mu \sim T^{0.76}$ has been assumed. The wall stress is then obtained by

$$\tau_w = c_f\tfrac{1}{2}\rho U^2 \tag{6}$$

The subscript appended to τ_w indicates the flow in which the stress is evaluated. For example, $\tau_{w\infty 2}$ denotes the stress on the wall exposed to the secondary freestream; τ_{w1} denotes the stress on the wall exposed to the quasi-one-dimensional-averaged primary stream.

Governing Equations

Having established approximate relations for the wall and dividing-streamline shear stresses, we now proceed to development of the governing equations. It is assumed that the flow is fully developed turbulent and that the layer is thin enough for the usual boundary-layer approximations to hold. Furthermore, the turbulent Prandtl number is taken to be unity, $Pr_t = 1$. The conservation equations for momentum and energy are

$$\bar{\rho}\frac{D\bar{u}}{Dt} = \frac{\partial}{\partial y}\left(\mu_t\frac{\partial\bar{u}}{\partial y}\right) = \frac{\partial\tau}{\partial y} \tag{7}$$

$$\bar{\rho}\frac{D\bar{H}}{Dt} = \frac{\partial}{\partial y}\left(\mu_t\frac{\partial\bar{H}}{\partial y}\right) = \frac{\partial q}{\partial y} \tag{8}$$

where

$$\frac{D}{Dt} \equiv \frac{1}{\bar{\rho}}\left(\overline{\rho u}\frac{\partial}{\partial x} + \overline{\rho v}\frac{\partial}{\partial y}\right)$$

μ_t is the eddy viscosity. Note that the previous equations hold for both the two-dimensional and axisymmetric configurations, provided that in the latter instance the layer thickness is small compared to the radius of the body,[9] in this case the cylinder defined by the dividing streamline. Comparison of the momentum and energy equations leads to the well-known Crocco–Busemann relation, which is cast here in terms of the freestream quantities:

$$\bar{H} = \frac{U_{\infty 1}H_{\infty 2} - U_{\infty 2}H_{\infty 1}}{U_{\infty 1} - U_{\infty 2}} + \frac{H_{\infty 1} - H_{\infty 2}}{U_{\infty 1} - U_{\infty 2}}\bar{u} \tag{9}$$

Inserting Eq. (9) in Eqs. (7) and (8), we derive a Reynolds' analogy relating the heat transfer to the shear stress on the dividing streamline:

$$q_* = \frac{H_{\infty 1} - H_{\infty 2}}{U_{\infty 1} - U_{\infty 2}}\tau_* \tag{10}$$

Strictly speaking, Eqs. (9) and (10) apply only for zero-pressure gradient. The pressure gradients encountered in this study are relatively mild, and so it is assumed that these equations still provide a good approximation.

We now derive the equations of motion for quasi-one-di-

Table 1 Parameters for the quasi-one-dimensional ejector model

Parameter	Axisymmetric	Two dimensional
A_1	πy_*^2	wy_*
A_2	$\pi(b^2 - y_*^2)$	$w(b - y_*)$
l_1	$y_*/2$	$wy_*/[2(y_* + w)]$
l_2	$(b - y_*)/2$	$w(b - y_*)/[2(b - y_* + w)]$
τ_1	$-\tau_*$	$-\tau_* l_1/y_* - 2\tau_{w1} l_1/w$
τ_2	$\tau_* y_*/(b + y_*) - \tau_{w\infty 2} b/(b + y_*)$	$(\tau_* - \tau_{w\infty 2}) l_2/(b - y_*) - 2\tau_{w2} l_2/w$
q_1	$-q_*$	$-q_* l_1/y_*$
q_2	$q_* y_*/(b + y_*)$	$q_* l_2/(b - y_*)$

mensional flow through a channel of arbitrary cross section. The following length scale is important:

$$l = \frac{\text{cross-sectional area}}{\text{wetted area per unit axial length}} \tag{11}$$

where wetted area means the surface area of the channel exposed to the fluid. For a simple shape, like a cylinder, the denominator in Eq. (11) is just the circumference. We consider a fixed control volume of cross-sectional area A and length dx. The mass conservation equation is

$$\frac{d\rho}{\rho} + \frac{dU}{U} + \frac{dA}{A} = 0 \tag{12}$$

The momentum equation (Newton's second law) gives

$$U\,dU + \frac{dp}{\rho} = \frac{\tau\,dx}{\rho l} \tag{13}$$

where τ represents all of the shear forces per unit wetted area. The energy equation is

$$dH = \frac{q}{\rho U l}\,dx \tag{14}$$

where q represents the heat flux per unit wetted area. The equation of state is

$$\frac{dp}{p} = \frac{d\rho}{\rho} + \frac{dT}{T} \tag{15}$$

In addition, the perfect gas assumption $h = c_p T$ holds. Equations (12–15) are combined to give a differential expression for velocity in terms of Mach number:

$$\frac{dU}{U} = \frac{1}{M^2 - 1}\left(\frac{dA}{A} + \frac{\tau\,dx}{pl} - \frac{q\,dx}{\rho U l h}\right) \tag{16}$$

which leads to a differential equation for the Mach number itself:

$$\frac{dM}{M} = \frac{1 + [(\gamma - 1)/2]M^2}{M^2 - 1}\left(\frac{dA}{A} + \frac{\tau\,dx}{pl}\right) - \frac{M(1 + \gamma M^2)}{2(M^2 - 1)}\frac{q\,dx}{\rho U l h} \tag{17}$$

Equations (11–17) are applicable to any cross-sectional geometry. For the ejector, they can be specialized to a particular stream by placing the appropriate subscript (1 or 2) under each variable. In the axisymmetric case, control volume 1 (primary stream) has a circular cross section while control volume 2 (secondary stream) has an annular cross section. For the two-dimensional ejector, both control volumes are rectangular. In formulating τ and q, the entire wetted area must be considered, even though the actual stresses and heat transfer may act only on a portion of it (they are averaged over the entire area). For example, the wetted area per unit axial length of the secondary stream of the axisymmetric ejector is $2\pi(b + y_*)$. The heat transfer q_* acts only on the inner surface $2\pi y_*$, therefore, the averaged heat transfer is $q_2 = q_* y_*/(b + y_*)$. Table 1 presents relations for the length scales, stresses, and heat fluxes for each stream of the axisymmetric and two-dimensional ejectors.

Solution Method

For prescribed initial conditions at $x = 0$, the quasi-one-dimensional solution of the flowfield depends only on the location of the dividing streamline $y_*(x)$. The shape of the dividing streamline is found by requiring pressure continuity across it, i.e., $p_1 = p_2$ at each x location. Starting at $x = 0$, we choose a slope dy_*/dx, a static pressure $p_{i1} = p_{i2}$, and a secondary-stream Mach number M_{i2} slightly above M_a. Let us first concentrate on stream 1. Since the conditions at $x = 0$ are known, the stress τ_1 and heat transfer q_1 are computed according to Table 1 and Eqs. (2) and (10). Equations (16) and (17) are integrated numerically over a small distance dx, yielding M_1, U_1, and the speed of sound $a_1 = U_1/M_1$ at the new location $x = dx$. The new area A_1 is calculated from Table 1. The pressure at $x = dx$ is then obtained from the integral mass conservation equation:

$$p_1 = \frac{\dot{m}_1 a_1}{\gamma_1 M_1 A_1}$$

The same procedure is then followed for stream 2, yielding a pressure p_2 at $x = dx$. If p_1 and p_2 are unequal, a new dy_*/dx is selected and the integration started anew until the difference $|p_1 - p_2|/p_1$ is of order 10^{-6}. A Newton–Raphson iteration technique is used for fast convergence. Once the new pressure has been calculated, we refer to the y-dependent model to obtain the freestream quantities ($U_{\infty 1}$, $U_{\infty 2}$, etc.) from the well-known isentropic relations. The new stresses and heat fluxes are then computed. Integration is advanced to the next x location and the entire iteration procedure is repeated.

As the integration progresses in x, the static pressure rises, and consequently the freestream Mach numbers decrease. If the secondary freestream Mach number $M_{\infty 2}$ becomes equal to the flight Mach number M_a and the ejector exit has not been reached, the integration is stopped and restarted at $x = 0$ with a higher value of M_{i2}. This step is repeated until $M_{\infty 2} = M_a$ at the ejector exit. By matching the two Mach numbers at $x = L$, we satisfy equality of the static pressures at the ejector exit and in the ambient stream. Now the solution is complete and all of the relevant information on thrust, mass pumping, etc., can be extracted. A Fortran program was written to perform the computation on a Pentium computer. Each flow case took about 30 s to compute.

Entropy Production

The entropy change in each stream is described by the basic thermodynamic relationship:

$$ds = \frac{1}{T}\left(dh - \frac{dp}{\rho}\right)$$

Using the momentum equation (13) and energy equation (14), the previous relation becomes

$$\frac{ds}{dx} = \frac{1}{\rho U l T}(q - U\tau) \tag{18}$$

from which we obtain $\dot{S} = \dot{m}\Delta s$. Summing up for the two streams, we have

$$\frac{d}{dx}(\dot{S}_1 + \dot{S}_2) = \frac{A_1}{T_1 l_1}(q_1 - U_1\tau_1) + \frac{A_2}{T_2 l_2}(q_2 - U_2\tau_2) \tag{19}$$

To put entropy rise in more practical terms, we define the equivalent total-pressure ratio, p_T/p_{Ti}, which is the ratio of the total pressure at $x = 0$ (unmixed conditions) to the total pressure at a downstream location x in a single adiabatic stream with mass flux $\dot{m}_1 + \dot{m}_2$ and entropy flux given by Eq. (19):

$$\frac{p_T}{p_{Ti}} \equiv \exp\left[-\frac{\dot{S}_1 + \dot{S}_2}{(\dot{m}_1 + \dot{m}_2)R}\right] \tag{20}$$

Thrust Augmentation

Based on the control volume depicted in Fig. 1, and on the assumptions of the analytical model stated earlier, the thrust of the ejector is

$$F_{\text{ejector}} = p_a[A_{e1}(1 + \gamma M_{e1}^2) + A_{e2}(1 + \gamma M_{e2}^2) - (A_e - A_{i1})(1 + \gamma M_a^2)] - \int_0^L \tau_{wa}(x)C\,dx \tag{21}$$

where the last term represents the skin friction on the outer surface of the ejector shroud, C being the shroud circumference. The ejector thrust is compared to the thrust of a sole jet operating at the same conditions as the primary ejector stream, that is, the same M_{i1}, p_{i1}, and A_{i1}:

$$F_{\text{jet}} = p_{i1}A_{i1}(1 + \gamma M_{i1}^2) \tag{22}$$

Since $p_{i1} < p_a$, the reference jet would be slightly overexpanded. Thrust augmentation is defined here as

$$\phi = \frac{F_{\text{ejector}} - F_{\text{jet}}}{F_{\text{jet}}} \tag{23}$$

Results and Discussion

Results are presented first for the baseline geometries shown in Fig. 2. The dimensions are chosen such that axisymmetric (A/S) and the two-dimensional (2D) ejectors share the same inlet areas for the primary and secondary streams. The primary Mach number is $M_{i1} = 2.0$, primary total temperature is $T_{Ti1} = 1200$ K, the ambient temperature is 300 K, and the ambient pressure is 1 atm. Figure 3 shows the static and total pressure distributions through the A/S ejector for flight Mach number $M_a = 0.2$ and ejector length $L/b = 10$. The static pressure is low at the inlet and rises to the ambient value at the exit, as the analytical model requires. The equivalent total pressure suffers a significant loss of about 50%. The p_T calculation depicted in Fig. 3 was done for inviscid walls to emphasize the effect of mixing alone on entropy rise. Including the effect of wall stresses would increase losses by a few percent. Although the total pressure loss is irrelevant to the thrust of a constant-area ejector, it would adversely effect the thrust of an ejector–diffuser combination where the expanding diffuser is used to further augment the thrust. Figure 4 depicts the freestream and quasi-one-dimensional-averaged Mach number distributions. The primary (supersonic) average Mach number M_1 decreases mainly because of the negative dividing-streamline shear stress acting on the primary stream. The average Mach number of the secondary (subsonic) stream M_2 is virtually constant, indicating that the effects of the stresses, area variation, and heat transfer on M_2 cancel each other out in this case. Both freestream Mach numbers drop because of the adverse pressure gradient, with $M_{\infty 2}$ reaching the value of M_a at the ejector exit, as the model requires. Figure 5 shows the shape of the dividing streamline and of the shear-layer edges. The edges are defined by adding and subtracting one half of the vorticity thickness [Eq. (3)] to the dividing streamline location. The dividing streamline is tilted towards the secondary stream. The corresponding plots for the two-dimensional ejector are very similar, and so they are omitted.

Figure 6 presents the thrust augmentation ϕ vs ejector length for the baseline geometries of Fig. 2 and for $M_a = 0.2$. Comparisons are made between the A/S and two-dimensional configurations with inviscid or viscous walls. With inviscid walls, the A/S and two-dimensional ejectors give virtually the same

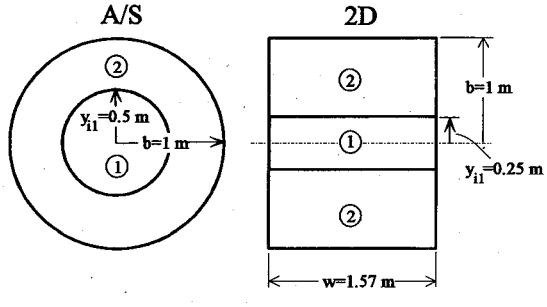

Fig. 2 Cross-sectional geometries of the axisymmetric (A/S) and two-dimensional (2D) baseline ejector configurations.

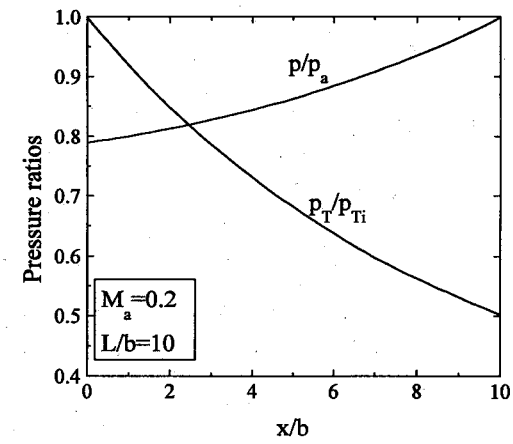

Fig. 3 Static and total pressure distributions in the axisymmetric baseline ejector.

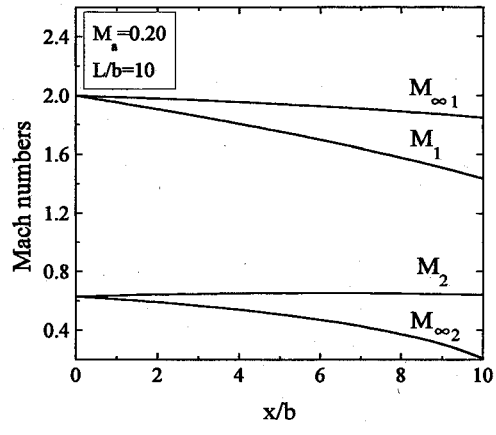

Fig. 4 Mach number distributions in the axisymmetric baseline ejector.

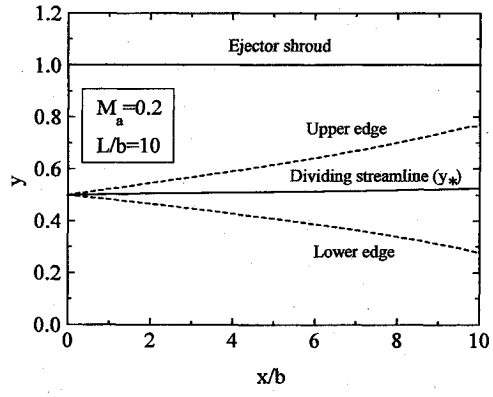

Fig. 5 Shear-layer geometry for the axisymmetric baseline ejector.

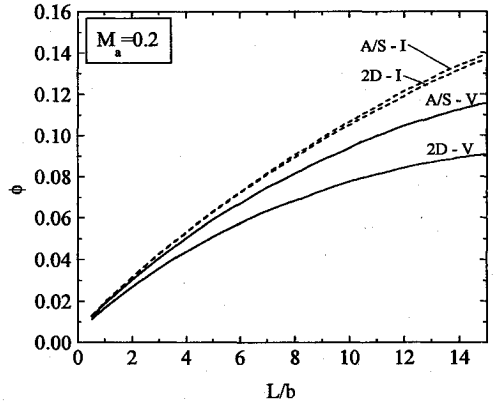

Fig. 6 Thrust augmentation vs ejector length for the axisymmetric (A/S) and two-dimensional (2D) baseline ejectors with inviscid (I) or viscous (V) walls.

performance. With wall stresses included, thrust augmentation drops by about 18% for the A/S ejector and 35% for the two-dimensional ejector. The two-dimensional ejector suffers from higher frictional losses because of the larger wetted area of the shroud and because the inner surfaces of the shroud sidewalls are exposed to the high stresses of the supersonic boundary layer of the primary stream. In contrast, the inner surface of the A/S ejector is exposed only to the low stresses of the subsonic boundary layer of the secondary stream. For both A/S and two-dimensional configurations with wall stresses, increasing the ejector length beyond a certain value yields a marginal rise in thrust augmentation. The comparison between viscous and inviscid walls suggests that one should be careful in evaluating inviscid thrust measurements, for example, measurements based on the pressure distribution around the ejector's inlet, because they may not fully account for the boundary-layer losses.

Figure 7 shows the dependence of thrust augmentation on M_a for the A/S and two-dimensional baseline ejectors with variable length. All configurations experience the same trend: thrust augmentation decreases with increasing M_a and becomes nil when M_a reaches about 0.7. Beyond that Mach number, the ejector is no longer pumping fluid and would cause a thrust deficit. The dependence of ϕ on secondary-to-primary area ratio is depicted in Fig. 8 for the baseline ejectors with variable b. At zero flight Mach number, ϕ increases slowly with area ratio. At higher M_a, ϕ becomes virtually independent of area ratio.

Mixing enhancement is often applied at the exit of the primary jet, typically using lobe mixers, to increase the shear-layer mixing, hence, improving the ejector performance.[4,5] Mixing enhancement can be partly modeled by raising the value of K in Eq. (2), which leads to proportional increases in $\tau*$, $q*$, and the growth rate. The dependence of thrust augmentation on K is shown in Fig. 9. Predictably, thrust increases with K almost linearly, the effect being more prominent at low flight Mach numbers. One must interpret these results with caution, however. First, the unavoidable thrust penalty of mixing enhancement devices is not included. Second, the assumption that K stays at the enhanced value throughout the length of the ejector seems weak for long ejectors. More likely, K is increased in the near field, but then decays to the unenhanced value of around 0.013 in the far field. Therefore, Fig. 9 serves as a guide as to the effect of ideal mixing enhancement, but the adverse effects just mentioned must be included for realistic predictions.

To assess the accuracy of the model, comparisons are made with the experimental measurements of Krothapalli et al.[3] The ejector of Ref. 3 was two dimensional with y_{i1} = 5.35 mm, b = 16 mm, and w = 47 mm. The primary Mach number was

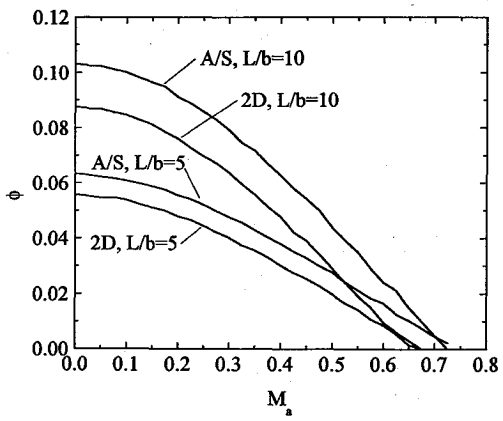

Fig. 7 Thrust augmentation vs flight Mach number.

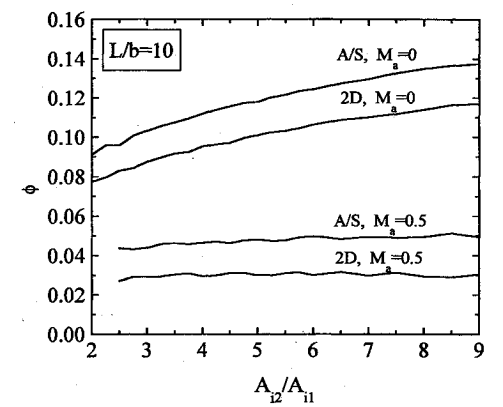

Fig. 8 Effect of area ratio on thrust augmentation.

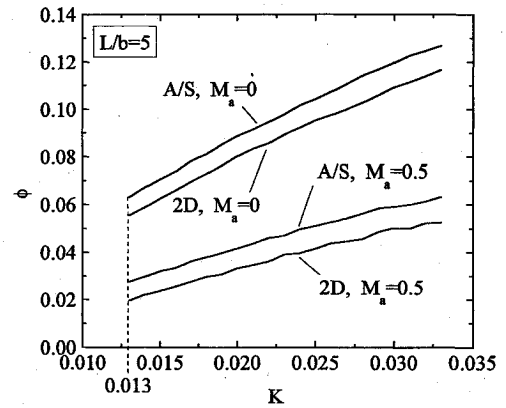

Fig. 9 Effect of ideal mixing enhancement on thrust augmentation.

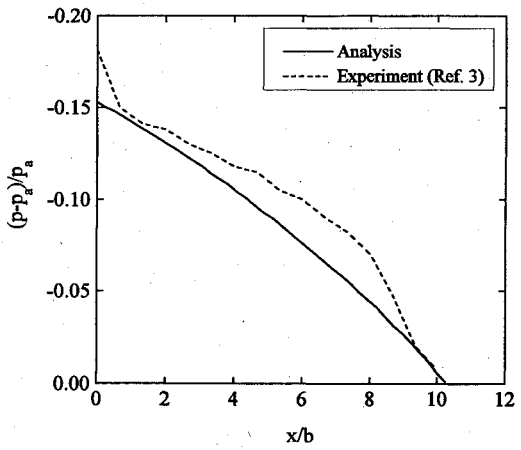

Fig. 10 Pressure distribution for the geometry and inlet conditions of the experiment of Ref. 3.

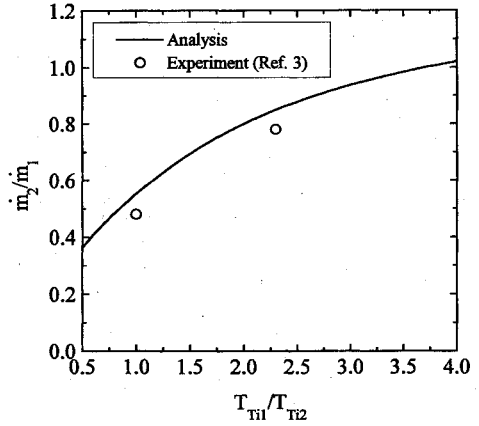

Fig. 11 Ejector pumping vs total-temperature ratio for the dimensions and inlet conditions of the experiment of Ref. 3.

M_{i1} = 1.47, the ambient air was quiescent (M_a = 0), and the primary total temperature was variable. No mixing enhancement was applied. The edges of the shear layer, calculated here using the vorticity thickness, do not reach either the shroud or the centerline of the ejector, hence, the assumptions of the quasi-one-dimensional model hold. We compare with the pressured-matched cases of Ref. 3 (total pressure ratio of 3.0). Figure 10 depicts the pressure distribution calculated by the model and the one measured experimentally with T_{Ti1}/T_{Ti2} = 1. The peak negative pressure predicted by the model is within 15% of the experimental value. The overall agreement between analytical and experimental pressure distributions is quite favorable. Next, Fig. 11 presents comparisons between the analytical and experimental mass flow ratios, plotted vs total-temperature ratio. Again, there is good agreement between model and experiment.

Conclusions

This relatively simple model, treating the two ejector streams as being quasi-one-dimensional, gives reasonable results on ejector performance, and could become a useful tool for optimizing ejector configurations before doing full-scale experimental or computational studies. The model predictions suggest that static thrust augmentation of 10% is not infeasible, but augmentation well above that figure would be hard to achieve in a practical system. The inherently smaller skin friction losses of the axisymmetric ejector make it a better performer than the two-dimensional ejector. For all ejector lengths and geometries, thrust augmentation becomes nil at a flight Mach number of around 0.7. Total-pressure loss because of mixing is significant and would adversely impact the thrust of an ejector–diffuser combination. The results compare favorably with available experimental data on pressure distributions and mass-flow ratios.

References

[1]von Kármán, T., "Theoretical Remarks on Thrust Augmentation," *Contributions to Applied Mechanics*, J.W. Edwards, Ann Arbor, MI, 1949.

[2]McCormick, B. W., "Aerodynamics of V-STOL Flight," Academic, New York, 1967, p. 282.

[3]Krothapalli, A., Ross, C., Yamamoto, K., and Joshi, M. C., "Fluid-Acoustic Interaction in a Low Area Ratio Supersonic Jet Ejector," AIAA Paper 93-4346, Oct. 1993.

[4]Tillman, T. G., Paterson, R. W., and Presz, W. M., "Supersonic Nozzle Mixer Ejector," *Journal of Propulsion and Power*, Vol. 8, No. 2, 1992, pp. 513–519.

[5]Narayanan, A. K., and Damodaran, K. A., "Supersonic-Ejector Characteristics Using a Petal Nozzle," *Journal of Propulsion and Power*, Vol. 10, No. 5, 1994, pp. 742–744.

[6]Papamoschou, D., "Model for Entropy Production and Pressure Variation in Confined Turbulent Mixing," *AIAA Journal*, Vol. 31, No. 9, 1993, pp. 1643–1650.

[7]Wygnanski, I., and Fiedler, H. E., "The Two-Dimensional Mixing Region," *Journal of Fluid Mechanics*, Vol. 41, 1973, pp. 327–361.

[8]Van Driest, E. R., "Turbulent Boundary Layer in Compressible Fluids," *Journal of the Aeronautical Sciences*, Vol. 18, 1951, pp. 145–160.

[9]White, F. M., "Viscous Fluid Flow," 1st ed., McGraw–Hill, New York, 1974, p. 339.